Small molecule inhibits α-synuclein aggregation, disrupts amyloid fibrils, and prevents degeneration of dopaminergic neurons

Jordi Pujols[a,b,1], Samuel Peña-Díaz[a,b,1], Diana F. Lázaro[c,d,e], Francesca Peccati[f,g], Francisca Pinheiro[a,b], Danilo González[f], Anita Carija[a,b], Susanna Navarro[a,b], María Conde-Giménez[h,i], Jesús García[j], Salvador Guardiola[j], Ernest Giralt[j,k], Xavier Salvatella[j,l], Javier Sancho[h,i], Mariona Sodupe[f,l], Tiago Fleming Outeiro[c,d,e,m,n], Esther Dalfó[b,o,p], and Salvador Ventura[a,b,l,2]

[a]Institut de Biotecnologia i Biomedicina, Universitat Autònoma de Barcelona, 08193 Bellaterra, Spain; [b]Departament de Bioquímica i Biologia Molecular, Universitat Autònoma de Barcelona, 08193 Bellaterra, Spain; [c]Department of Experimental Neurodegeneration, University Medical Center Göttingen, 37073 Göttingen, Germany; [d]Center for Biostructural Imaging of Neurodegeneration, University Medical Center Göttingen, 37073 Göttingen, Germany; [e]Center for Nanoscale Microscopy and Molecular Physiology of the Brain, University Medical Center Göttingen, 37073 Göttingen, Germany; [f]Departament de Química, Universitat Autònoma de Barcelona, 08193 Bellaterra, Spain; [g]Laboratoire de Chimie Théorique, Sorbonne Universités, CNRS, F-75005 Paris, France; [h]Department of Biochemistry and Molecular and Cell Biology, University of Zaragoza, 50018 Zaragoza, Spain; [i]Institute for Biocomputation and Physics of Complex Systems (BIFI), University of Zaragoza, 50018 Zaragoza, Spain; [j]Institute for Research in Biomedicine (IRB Barcelona), The Barcelona Institute of Science and Technology (BIST), 08028 Barcelona, Spain; [k]Department of Inorganic and Organic Chemistry, University of Barcelona, 08028 Spain; [l]Institució Catalana de Recerca i Estudis Avançats (ICREA), 08010 Barcelona, Spain; [m]Max Planck Institute for Experimental Medicine, 37075 Göttingen, Germany; [n]Institute of Neuroscience, The Medical School, Newcastle University, Newcastle upon Tyne NE2 4HH, United Kingdom; [o]Faculty of Medicine, University of Vic-Central University of Catalonia (UVic-UCC), 08500 Vic, Spain; and [p]Institut de Neurociències, Universitat Autònoma de Barcelona, 08193 Bellaterra, Spain

Edited by Gregory A. Petsko, Weill Cornell Medical College, New York, NY, and approved August 16, 2018 (received for review April 3, 2018)

Parkinson's disease (PD) is characterized by a progressive loss of dopaminergic neurons, a process that current therapeutic approaches cannot prevent. In PD, the typical pathological hallmark is the accumulation of intracellular protein inclusions, known as Lewy bodies and Lewy neurites, which are mainly composed of α-synuclein. Here, we exploited a high-throughput screening methodology to identify a small molecule (SynuClean-D) able to inhibit α-synuclein aggregation. SynuClean-D significantly reduces the in vitro aggregation of wild-type α-synuclein and the familiar A30P and H50Q variants in a sub-stoichiometric molar ratio. This compound prevents fibril propagation in protein-misfolding cyclic amplification assays and decreases the number of α-synuclein inclusions in human neuroglioma cells. Computational analysis suggests that SynuClean-D can bind to cavities in mature α-synuclein fibrils and, indeed, it displays a strong fibril disaggregation activity. The treatment with SynuClean-D of two PD *Caenorhabditis elegans* models, expressing α-synuclein either in muscle or in dopaminergic neurons, significantly reduces the toxicity exerted by α-synuclein. SynuClean-D–treated worms show decreased α-synuclein aggregation in muscle and a concomitant motility recovery. More importantly, this compound is able to rescue dopaminergic neurons from α-synuclein–induced degeneration. Overall, SynuClean-D appears to be a promising molecule for therapeutic intervention in Parkinson's disease.

Parkinson's disease | α-synuclein | protein aggregation | aggregation inhibition | dopaminergic degeneration

Parkinson's disease (PD) is the second most prevalent neurodegenerative disorder after Alzheimer's disease (AD) and is still incurable (1). PD is the most common synucleinopathy, a group of neurodegenerative disorders that includes dementia with Lewy bodies and multiple system atrophy (MSA), among others (2, 3). Although the synucleinopathies are multifactorial disorders, the molecular events triggering the pathogenic breakthrough of the disease converge to the abnormal aggregation of α-synuclein (α-Syn) in dopaminergic neurons (4, 5). α-Syn aggregation also occurs in oligodendrocytes in patients with MSA (6). α-Syn is an intrinsically disordered protein, which is expressed at high levels in the brain. α-Syn function is thought to be related to vesicle trafficking (7). This wild-type protein is the main component of cytoplasmic Lewy bodies (LB) and Lewy neurites (LN) in sporadic PD (8). In addition, dominantly inherited mutations in α-Syn, as well as multiplications of the gene encoding for α-Syn (*SNCA*), cause familial forms of PD (9).

Interfering with α-Syn aggregation has been envisioned as a promising disease-modifying approach for the treatment of PD (1). However, the disordered nature of α-Syn precludes the use of structure-based drug design for the discovery of novel molecules able to modulate α-Syn aggregation. Therefore, many efforts have focused on the analysis of large collections of chemically diverse molecules to identify lead compounds (10). Recently, we have developed an accurate and robust high-throughput screening methodology to identify α-Syn aggregation inhibitors (11). Here, we describe the properties of SynuClean-D (SC-D), a small molecule identified with this approach (*SI Appendix*, Fig. S1). We first performed a detailed in vitro biophysical characterization of the inhibitory and disaggregation activities of SC-D and tested its performance in human neural cells. Finally, we validated the effects in vivo in two well-established *Caenorhabditis elegans* models of PD, which express α-Syn either in muscle cells or in dopaminergic

Significance

Parkinson's disease is characterized by the accumulation of amyloid deposits in dopaminergic neurons, mainly composed of the protein α-synuclein. The disordered nature of α-synuclein and its complex aggregation reaction complicate the identification of molecules able to prevent or revert the formation of these inclusions and the subsequent neurodegeneration. By exploiting a recently developed high-throughput screening assay, we identified SynuClean-D, a small compound that inhibits α-synuclein aggregation, disrupts mature amyloid fibrils, prevents fibril propagation, and abolishes the degeneration of dopaminergic neurons in an animal model of Parkinson's disease.

Author contributions: S.V. designed research; J.P., S.P.-D., D.F.L., F. Peccati, F. Pinheiro, D.G., A.C., S.N., M.C.-G., J.G., S.G., and E.D. performed research; J.P., S.P.-D., D.F.L., E.G., X.S., J.S., M.S., T.F.O., E.D., and S.V. analyzed data; and M.S., E.D., and S.V. wrote the paper.

Conflict of interest statement: J.P., S.P.-D., M.C.-G., J.S., E.D., and S.V. are inventors on a patent application (PCT/EP2018/054540) related to the compound in this study.

This article is a PNAS Direct Submission.

[1]J.P. and S.P.-D. contributed equally to this work.

[2]To whom correspondence should be addressed. Email: salvador.ventura@uab.es.

This article contains supporting information online at www.pnas.org/lookup/suppl/doi:10.1073/pnas.1804198115/-/DCSupplemental.

Published online September 24, 2018.

neurons. The inhibitor reduced α-Syn aggregation, improved motility, and protected against neuronal degeneration.

Results

SynuClean-D Inhibits α-Syn Aggregation in Vitro. The formation of α-Syn amyloid fibrils can be reproduced in vitro by incubating the recombinant protein. However, fibril growth is very slow and highly variable, complicating drug screening (12). We have implemented a robust high-throughput kinetic assay to screen large chemical libraries in the search for α-Syn aggregation inhibitors (11). The assay uses thioflavin-T (Th-T) as readout of amyloid formation, completing highly reproducible reactions in 30 h. Approximately 14,400 chemically diverse compounds of the HitFinder Collection from Maybridge were screened with this approach. SC-D [2-hydroxy-5-nitro-6-(3-nitrophenyl)-4-(trifluoromethyl)nicotinonitrile], a small aromatic compound, was identified as one of the molecules of potential interest (*SI Appendix*, Fig. S1). Many compounds with promising pharmacological characteristics never become drugs because they are rapidly metabolized in the liver and therefore have low oral bioavailability. SC-D was metabolically stable in the presence of human hepatic microsomes, with an intrinsic clearance of <5 $\mu L \cdot min^{-1} \cdot mg^{-1}$ (*SI Appendix*, Fig. S2).

Incubation of 70 μM α-Syn with 100 μM SC-D impacted α-Syn aggregation, as monitored by Th-T fluorescence (Fig. 1*A*). The analysis of the aggregation curves indicated that the autocatalytic rate constant in the presence of the compound (k_a 0.25 h^{-1}) was 25% lower than in its absence (k_a 0.33 h^{-1}). SC-D increases t_{50} by 1.5 h and reduces by 53% the amount of Th-T–positive material at the end of the reaction. By measuring light scattering, we confirmed that the observed changes in Th-T fluorescence reflected an effective decrease in the levels of α-Syn aggregates, with a reduction of 48 and 58% in the scattering signal at the end of the reaction in the presence of SC-D when exciting at 300 and 340 nm, respectively (Fig. 1*B*). Nanoparticle tracking analysis indicated that the presence of SC-D increased the number of particles of <100 nm and decreased the formation of large aggregates (150 to 500 nm) (*SI Appendix*, Fig. S3). Finally, transmission electron microscopy (TEM) images confirmed that samples incubated with SC-D contained smaller and much fewer fibrils per field than untreated samples (Fig. 1 *C* and *D*). The inhibitory activity of SC-D was dose-dependent and still statistically significant at 10 μM (1:7 compound:α-Syn ratio), where it reduces the final Th-T signal by 34% (Fig. 1*E*).

We further investigated whether SC-D was active against the aggregation of α-Syn variants associated with PD (1). SC-D was able to reduce by 45 and 73% the amount of Th-T–positive aggregates at the end of the reaction for the H50Q and A30P α-Syn familial variants, respectively (Fig. 1*F*).

The inhibitory activity of SC-D was also assessed using protein-misfolding cyclic amplification (PMCA) (13). Conceptually based on the nucleation-dependent polymerization model for prion replication, PMCA has been recently adapted to amplify α-Syn amyloid fibrils (14). The PMCA technique combines cycles of incubation at 37 °C, to grow fibrils, and sonication, to break fibrils into smaller seeds. In our conditions, a single cycle of amplification was sufficient to generate amyloid-like protease K (PK)-resistant α-Syn assemblies, but the highest levels of protection were attained after four rounds (Fig. 1*G*). When the same experiment was performed in the presence of SC-D, we observed a substantial decrease in the amount of PK-resistant material (Fig. 1*H*), indicating that the molecule was interfering with α-Syn template seeding amyloid formation.

SynuClean-D Disrupts Preformed α-Syn Fibrils. The progress of α-Syn PMCA reactions can also be monitored by using the Th-T signal as the readout for fibril assembly (15). Consistent with PK resistance analysis, Th-T fluorescence of α-Syn increased significantly after four cycles of PMCA (Fig. 2*A*). Surprisingly, in the presence of SC-D, the Th-T signal not only did not increase, but

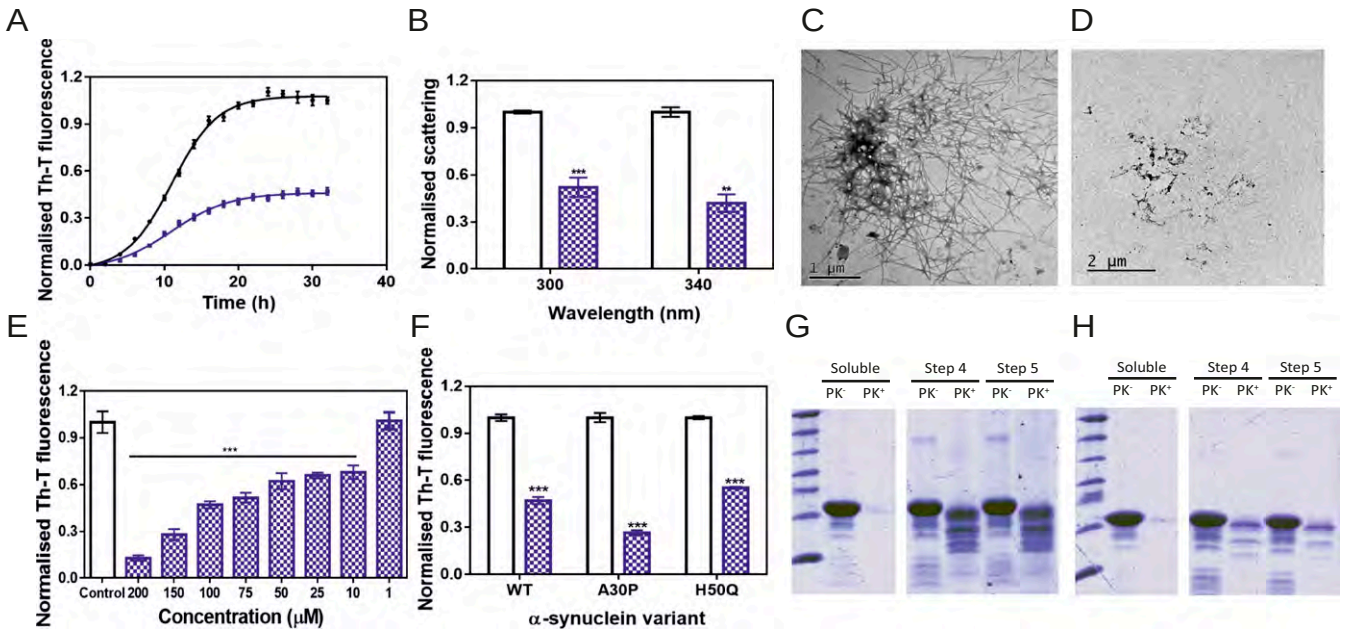

Fig. 1. Effect of SynuClean-D on the aggregation of α-Syn in vitro. (*A*) α-Syn aggregation kinetics in the absence (black) and presence (blue) of SC-D followed by Th-T–derived fluorescence. (*B*) Light-scattering signal at 300 and 340 nm, both in the absence (white) and presence (blue) of SC-D. (*C* and *D*) Representative TEM images in the absence (*C*) and presence (*D*) of SC-D. (*E*) Inhibition of α-Syn aggregation in the presence of different concentrations of SC-D. (*F*) H50Q and A30P α-Syn variant aggregation in the absence (white) and presence (blue) of SC-D. (*G* and *H*) Bis/Tris gels of PMCA samples in the absence (*G*) and presence (*H*) of SC-D, both analyzed after PK digestion. Soluble α-Syn and PMCA steps 4 and 5 are shown. Th-T fluorescence is plotted as normalized means. Final points were obtained at 48 h. Error bars are represented as SE of mean values; $^{**}P < 0.01$ and $^{***}P < 0.001$.

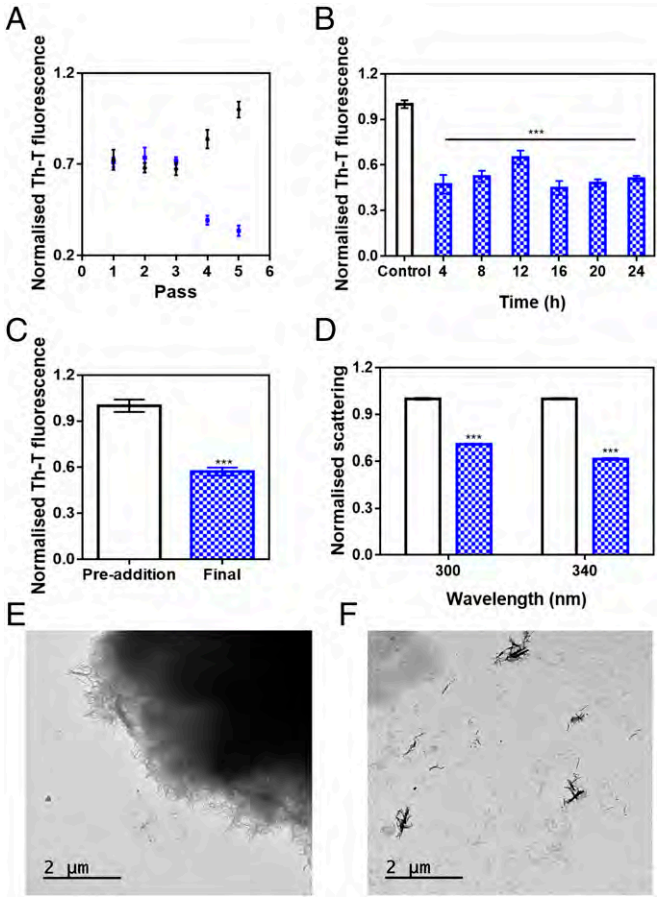

Fig. 2. Disaggregational capacity of SynuClean-D. (*A*) Th-T fluorescence of the different PMCA passes of both treated (blue) and untreated (black) samples with SC-D. (*B*) Aggregation kinetics of α-Syn after the addition of SC-D at different time points. (*C* and *D*) Th-T–derived fluorescence (*C*) and light-scattering (*D*) assays before and after the addition of SC-D to preformed α-Syn fibrils. (*E* and *F*) Representative TEM images in the absence (*E*) and presence (*F*) of SC-D. Th-T fluorescence is plotted as normalized means. Error bars are represented as SE of mean values; ***$P < 0.001$.

began to decrease after the third cycle. This suggested that SC-D might disrupt newly formed amyloid fibrils.

To address the time window in which SC-D is active, we set up aggregation reactions with a constant amount of SC-D at different time intervals. As presented in Fig. 2*B*, the effect of SC-D on the final amount of amyloid structures was independent of whether it was added at the beginning (4 h), in the middle (12 h), or at the end (18 h) of the exponential phase, or even when the reaction had already attained a plateau (24 h). These results suggested again ability to disrupt/destabilize fibrils.

To confirm the fibril-disrupting activity of SC-D, 4-d mature α-Syn fibrils were incubated in the absence or presence of the compound for 24 h. Incubation with SC-D promoted a 43% reduction in Th-T fluorescence emission (Fig. 2*C*). Moreover, light-scattering measurements indicated a reduction in the amount of detectable aggregates by 29 and 39% at 300 and 340 nm, respectively (Fig. 2*D*). Consistently, TEM images illustrated how 4-d-incubated α-Syn tended to form big fibrillary clusters (Fig. 2*E*), which became completely disrupted in the presence of SC-D (Fig. 2*F*).

α-Syn Fibrils Can Accommodate SynuClean-D. To assess if SC-D can bind monomeric and soluble α-Syn, the recombinant protein was isotopically labeled and NMR ^{1}H-^{15}N-HSQC spectra of 70 μM [^{15}N]α-Syn were recorded in the absence and presence of SC-D. We did not detect any perturbations in chemical shifts or peak intensities with respect to the original α-Syn spectrum in the presence of 100 μM concentration of the molecule (*SI Appendix*, Fig. S4), indicating that SC-D does not bind α-Syn monomers.

Induced-fit docking simulations of α-Syn–SC-D revealed four major poses for its interaction with α-Syn fibrils (16): two internal, with SC-D fully inserted in the fibril (poses 1 and 2), and two external, with SC-D partially exposed (poses 3 and 4) (*SI Appendix*, Fig. S5). In the internal poses, the ligand is sandwiched between two parallel β-sheets of the Greek-key motif and interacts with the side chains of ALA53, VAL55, THR59, GLU61, THR72, and GLY73. The only difference between pose 1 and 2 lies in the orientation of the compound in the binding pocket. PELE (17) interaction energies are stronger for the internal poses, where SC-D binds essentially through dispersion interactions into a solvent-excluded cavity, than for external ones, where SC-D inserts into a surface groove of the fibril. In light of these calculations, we predict that SC-D binds into the core of α-Syn fibrils.

MM/GBSA calculations (*SI Appendix*, Table S1) (18, 19) show that internal binding pose 1 (Fig. 3) exhibits the largest binding energy with the fibril, the computed ΔG_{bind} being -18.4 ± 4.1 kcal·mol^{-1}. The main contribution comes from the van der Waals term, representing roughly 80% of the interaction. This is not surprising given the nature of SC-D, a planar aromatic molecule. Plots of the reduced density gradient versus the density (*SI Appendix*, Fig. S6*A*) provide information on the nature of the noncovalent interactions in the system (20). Peaks in the negative and positive regions of the x axis are indicative of attractive and repulsive interactions, respectively. The region around zero corresponds to the weakest noncovalent van der Waals contacts. Though weak, these interactions are present in large number and involve the whole body of the molecule, being the largest contribution to the binding energy. Their spatial extension is shown in *SI Appendix*, Fig. S6*B*. For pose 1, the noncovalent interaction plot shows that

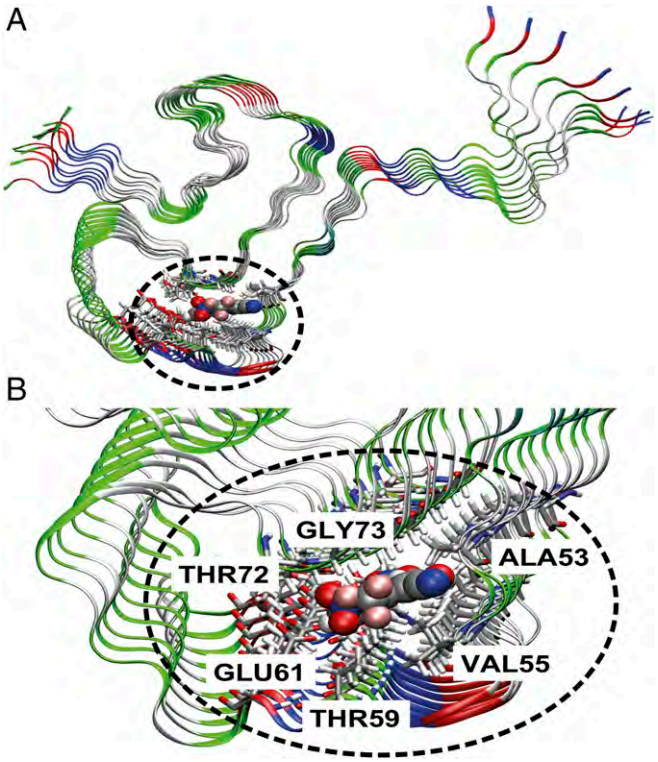

Fig. 3. Characterization of SynuClean-D–fibril interaction. General view (*A*) and zoom (*B*) of the most stable binding pose of SC-D on the α-Syn fibril model.

besides van der Waals, an H-bond contact is responsible for the binding of SC-D (*SI Appendix*, Fig. S6*A*).

SynuClean-D Inhibits the Formation of Intracellular α-Syn Aggregates in Cultured Cells. We tested the potential toxicity of SC-D for human neuroglioma (H4) and human neuroblastoma (SH-SY5Y) cells. For both cell lines, the molecule was innocuous at concentrations as high as 50 μM (Fig. 4*A* and *SI Appendix*, Fig. S7). We used a well-established cell model that enabled us to assess α-Syn inclusion formation. H4 cells were transiently transfected with C-terminally modified α-Syn (synT) and synphilin-1, which results in the formation of LB-like inclusions, as we previously described (9). The formation of α-Syn inclusions was assessed 24 h after treatment by immunofluorescence (Fig. 4*D*). Upon treatment with 1 and 10 μM SC-D, we observed a significant increase in the number of transfected cells devoid of α-Syn inclusions (SC-D, 1 μM: 42.4 ± 1.0%; SC-D, 10 μM: 49.5 ± 4.5%) relative to untreated samples (control: 28.7 ± 2.0%) (Fig. 4*B*). SC-D treatment also promoted a significant decrease in the number of transfected cells displaying more than five aggregates (SC-D, 1 μM: 35.5 ± 5.0%; SC-D, 10 μM: 32.5 ± 6.6%) relative to control cells (control: 49.6 ± 5.6%) (Fig. 4*C*).

SynuClean-D Inhibits α-Syn Aggregation in a *C. elegans* Model of PD. Next, we tested SC-D in a living system. We used a well-studied nematode model of PD, the strain NL5901, in which human α-Syn fused to the yellow fluorescent protein (YFP) is under control of the muscular *unc-54* promoter, transgene *pkIs2386* [*Punc-54::α-SYN::YFP*] (21). Muscle expression has been used successfully to model protein-misfolding diseases and to identify modifier genes without considering neuronal effects (21, 22). To determine the effects of SC-D in α-Syn accumulations, animals at the fourth larval stage (L4) (23) were incubated with and without the compound, to analyze the inhibitor efficiency in aged worms at 9 d posthatching (L4 + 7), which mimics aged human PD (24). We avoided a compound burst at L1 (25) because this treatment mimics a preventive rather than a disease-modifying intervention. Quantification of the number of α-Syn aggregates revealed that, in treated animals, the number of visible α-Syn aggregates decreased by 13.2 units, relative to untreated worms (18.3 ± 2.8 vs. 31.5 ± 1.1, respectively) (Fig. 5 *A* and *D*). In some animals, treatment resulted in a near-complete loss of protein aggregates (*SI Appendix*, Fig. S8). In this assay, SC-D is as effective as epigallocatechin gallate (EGCG), a polyphenol able to inhibit α-Syn aggregation and to disentangle preformed α-Syn aggregates (26, 27). EGCG has also been shown to reduce the deposits of the amyloid β-peptide in a *C. elegans* muscular model of AD (28). In our PD model, EGCG treatment reduced the number of visible aggregates by 13.4 units (18.1 ± 0.7) (Fig. 5*A*).

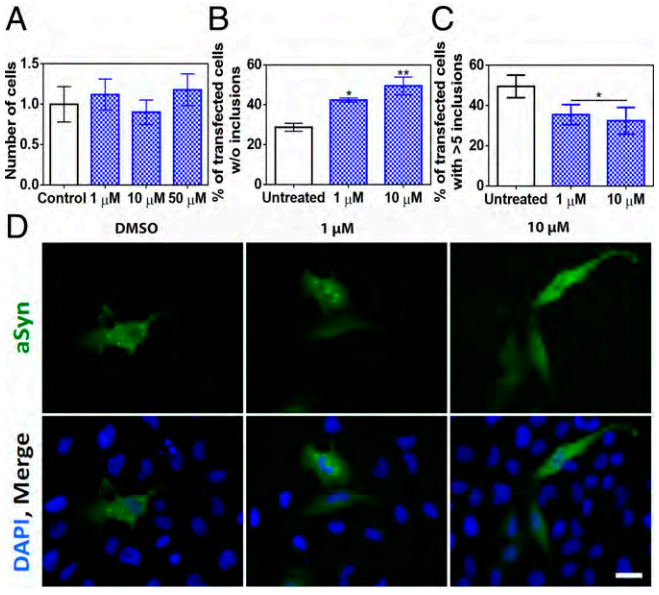

Fig. 4. Inhibition of α-Syn aggregate formation in cultured cells. (*A*) Human neuroglioma cell (H4) survival when incubated with different concentrations of compound (blue) and without (white) the compound. (*B* and *C*) Reduction of α-Syn inclusion formation in human cultured cells in the presence of different concentrations of SC-D. (*B*) Percentage of transfected cells devoid of α-Syn aggregates. (*C*) Percentage of transfected cells bearing >5 α-Syn aggregates. (*D*) Representative epifluorescent images from cells treated with SC-D. $n = 3$. (Scale bar, 30 μm.) Error bars are represented as SE of means; $^{*}P < 0.05$ and $^{**}P < 0.01$.

Major defects in regular bending have been used to identify modifiers of protein aggregation (21). Indeed, *C. elegans* thrashing can be measured in liquid media by counting the number of body bends per unit of time (29). By using this method, we confirmed an improved motility in SC-D–treated animals in comparison with nontreated worms (Fig. 5 *B* and *E*). We observed a decrease of bending of 72.2% in YFP::α-SYN animals compared with the N2 wild-type strain (18.1 ± 2.5 vs. 90.3 ± 6.7, respectively). This motility decrease was reverted in YFP::α-SYN animals treated with SC-D. In these animals, the average bending increased by 2.7-fold, compared with nontreated animals (18.1 ± 2.5 vs. 49.1 ± 4.4) (Movies S1 and S2).

SynuClean-D Prevents Degeneration of Dopaminergic Neurons in a *C. elegans* Model of PD. PD is characterized by the degeneration of dopaminergic (DA) neurons. There exist four pairs of DA neurons in *C. elegans* hermaphrodites, three of them (CEPD, CEPV, and ADE) located in the anterior part, and one pair, the PDE, in the posterior part of the nematode (30). To investigate the neuroprotective role of SC-D in dopaminergic cell death, we sought to analyze its effect in a *C. elegans* model of PD in which DA neurons undergo age-dependent neurodegeneration (31). In this model (strain UA196), animals express both human α-Syn and GFP in DA neurons, according to the simplified genotype *Pdat-1*::GFP; *Pdat-1*::α-SYN (the full genotype is detailed in *SI Appendix*). This strain has been successfully used for the investigation of human PD-related mechanisms (24). When human α-Syn is expressed in these animals' DA neurons, the six DA neurons within the anterior region of the worm display progressive degenerative characteristics (32). To model the aging contribution to PD, we determined the inhibitor capacity of SC-D in dealing with DA cell death induced by human α-Syn at 9 d (L4 + 7) posthatching. Cell bodies and neuronal processes were assessed to determine whether these structures displayed morphology changes. At 9 d posthatching, only 14.0 ± 1.5% of nontreated animals showed six wild-type DA neurons. In contrast, 44.4 ± 2.8% of treated animals showed the six intact DA neurons (Fig. 5 *C* and *F*), which evidenced the ability of SC-D to protect against α-Syn–induced DA neuron degeneration. In contrast to SC-D, the administration of EGCG did not have any beneficial impact on neurodegeneration, since only 12.0 ± 0.8% of EGCG-treated animals exhibited six intact DA neurons, a proportion that is fairly similar to that in untreated worms (14.0 ± 1.5%) (Fig. 5*C*).

Discussion

α-Syn aggregation plays a major pathophysiological role in the development of PD. Since its discovery and subsequent identification as the most abundant protein in Lewy bodies (3), α-Syn was shown to be important for a number of cellular processes (7). Therapeutic strategies targeting the aggregation of α-Syn thus hold the promise to result in disease modification and mitigate pathology in PD (33).

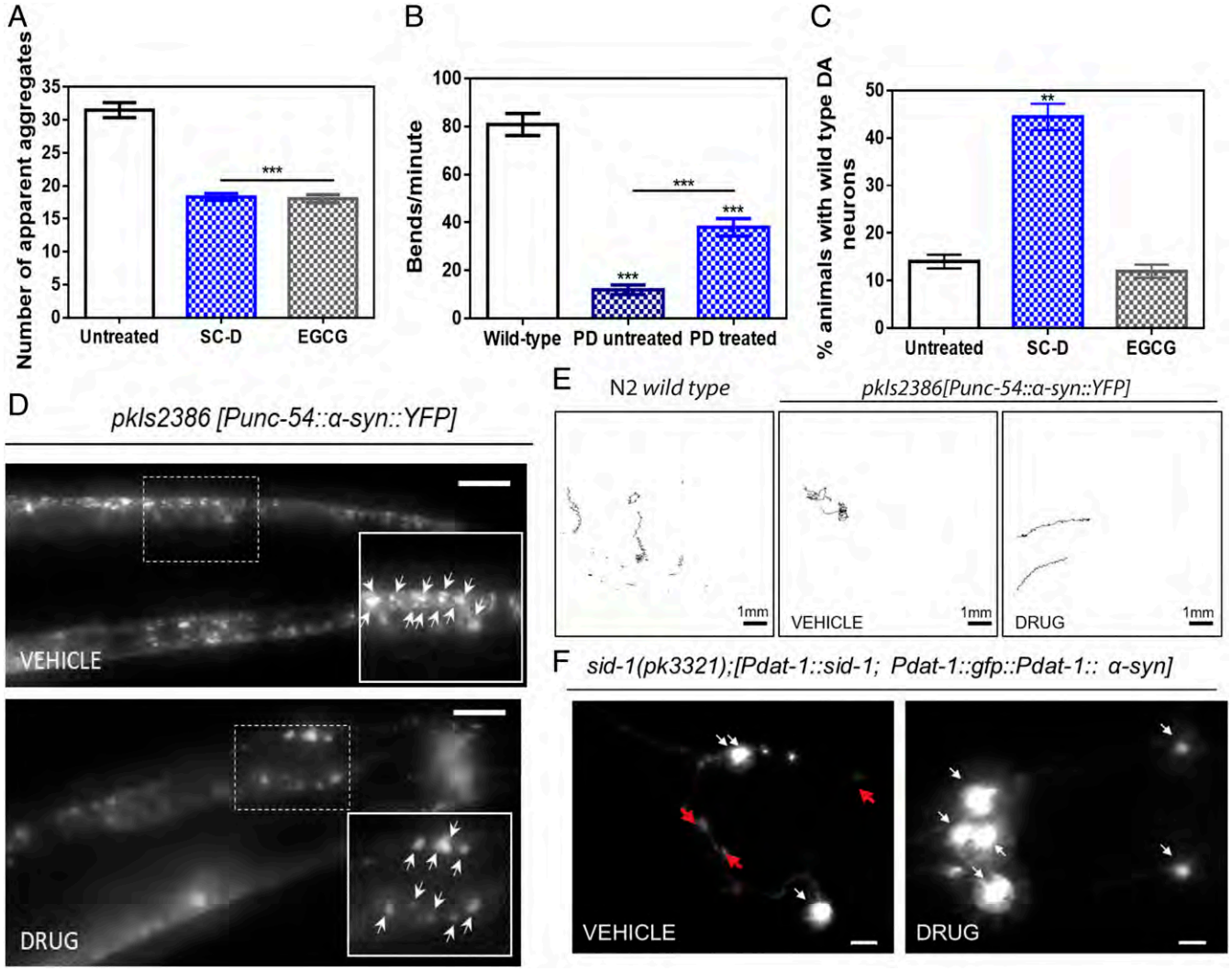

Fig. 5. Inhibition effect of the compound in the formation of α-Syn inclusions and protection from the α-Syn–induced dopaminergic cell death in *C. elegans* models of PD. (*A*) Quantification of α-Syn muscle inclusions per area of NL5901 worms in the absence (white) and presence of SC-D (blue) or EGCG (gray). (*B*) Worm-thrashing representation as the number of bends per minute of N2 wild-type and NL5901 worms treated without (white) and with SC-D (blue). (*C*) Percentage of UA196 worms that maintain a complete set of dopaminergic neurons (four pairs located in the head) after treatment without (white) and with SC-D (blue) or EGCG (gray) for 7 d after the L4 stage. (*D*) Representative images of α-Syn muscle aggregates obtained by epifluorescence microscopy of NL5901 worms treated without (*Top*, vehicle) and with SC-D (*Bottom*, drug). (Scale bars, 10 μm.) Between 40 and 50 animals were analyzed per condition. Aggregates are indicated by white arrows. (*E*) Path representation of the mobility of N2 wild-type (*Left*, vehicle) and NL5901 worms grown without (*Middle*, vehicle) and with SC-D (*Right*, drug). (Scale bars, 1 mm.) (*F*) Representative worms expressing GFP–α-Syn specifically in DA neurons without (*Left*, vehicle) and with SC-D (*Right*, drug) for 7 d after L4. Healthy neurons are labeled with white arrows, whereas neurodegenerated or missing neurons are labeled with red arrows. (Scale bars, 30 μm.) Between 40 and 50 animals were analyzed per condition in each experiment. Data are shown as means, and error bars are shown as the SE of means; $^{**}P < 0.01$ and $^{***}P < 0.001$.

The screening of large chemical libraries has rendered promising molecules that inhibit the progression of PD by targeting the aggregation of α-Syn, like BIOD303 (34) or anle138b (35). Here, by exploiting a previously developed high-throughput methodology, we identified SC-D as a metabolically stable compound able to inhibit >50% of α-Syn amyloid formation in vitro when employed in a 0.7:1 (protein:SC-D) ratio. The ability of SC-D to inhibit α-Syn aggregation was confirmed by light-scattering and TEM assays. SC-D was also active against the aggregation of α-Syn mutants that cause familial forms of the disease.

The activity of SC-D was concentration-dependent and still evident at a substoichiometric 7:1 protein:compound ratio. This already suggested that, unlike other compounds, SC-D does not bind to monomeric α-Syn, supported by NMR experiments. From a therapeutic perspective, this is an important advantage, as SC-D is not expected to interfere with the physiological functions of the soluble protein.

PMCA experiments indicated that SC-D might disrupt α-Syn amyloid assemblies, a property that was confirmed by the ability of SC-D to reduce the amount of formed amyloid fibrils, almost independent of the stage of the aggregation reaction at which it was added. Indeed, SC-D is very effective at disassembling clusters of aged α-Syn amyloid fibrils, conceptually similar to the α-Syn amyloid inclusions recurrently observed in the dopaminergic neurons of PD patients. This is important, because the disassembly of preformed amyloid fibrils has been traditionally challenging, and very few molecules have been reported to break down amyloid fibrils (27) because of their high stability. Computational analysis suggests that the disrupting activity of SC-D is mediated by its binding to an inner cavity in α-Syn fibrils. The disassembly of large fibrils has been seen traditionally as a risky strategy for the amelioration of aggregation-linked diseases, because it may increase the population of smaller toxic species

(12). However, our in vivo experiments demonstrate that this is not the case for SC-D.

The ability of SC-D to target preformed fibrils might have important implications for the prion-like pathological spreading of α-Syn aggregates in the brain (4). By disentangling transmissible fibrillary assemblies, SC-D might reduce templated seeding and thus aggregate-catalyzed conversion of soluble α-Syn molecules into their insoluble forms. It has been suggested that to attain a sustainable spreading and prevent dilution of aggregates as they propagate from cell to cell, a process of aggregate amplification is required, in addition to templated seeding (36). PMCA emulates these particular conditions in vitro. The potency of SC-D in blocking PMCA-induced amplification of α-Syn fibrils is thus promising.

SC-D displayed low toxicity for neural cells and displayed cellular permeability. Indeed, SC-D treatment at concentrations as low as 1 μM significantly reduced the number of α-Syn inclusions and the number of inclusions per cell. These data prompted us to assess the effects of SC-D treatment in in vivo models of α-Syn aggregation. First, we selected a well-validated *C. elegans* model of PD that expresses human α-Syn in muscular cells (21). When worms were treated with SC-D at preadult stages, we observed an important decrease in the number of α-Syn inclusions and a significant recovery of motility in adult PD worms. However, independent of whether a compound targets the early stages of aggregation or disrupts mature protein inclusions, or both, the final aim of a PD-oriented therapy is not to interfere with α-Syn aggregation per se but instead to prevent the neuronal degeneration associated with this phenomenon. It is in this therapeutic context where SC-D stands out, since it is able to increase by more than threefold the number of animals with intact DA neurons in a *C. elegans* model in which the expression of human α-Syn is directly connected to dopaminergic degeneration (31).

Conclusions

In the present study, we describe how drug-screening efforts have crystallized in the discovery of a molecule able to inhibit α-Syn aggregation, both in vitro and in vivo, without interacting significantly with functional, monomeric, and soluble α-Syn. SC-D is a nontoxic molecule that exhibits a unique capability to interact with and disassemble amyloid fibrils, a property that is likely connected to its ability to prevent the α-Syn–promoted degeneration of dopaminergic neurons. Taken together, SC-D constitutes a very promising lead compound for the development of a novel therapeutic molecule for disease modification in PD and other synucleinopathies.

Materials and Methods

Protein purification, metabolic stability assays, in vitro aggregation studies, protein-misfolding cyclic amplification, molecular dynamics simulations, NMR studies, cytotoxicity assays, in-cell aggregation studies, and the *C. elegans* models of PD are described in detail in *SI Appendix*.

ACKNOWLEDGMENTS. We thank the Infraestructura Científica y Técnica Singular NMR facility at Centres Científics i Tecnològics de la Universitat de Barcelona for help with NMR, Amable Bernabé at Institut de Ciència de Materials de Barcelona–Consejo Superior de Investigaciones Científicas for help with nanoparticle tracking analysis, and Anna Villar-Pique for help with plasmid construction. The worm strain UA196 used for neurodegeneration assays was a generous gift of Dr. Guy A. Caldwell. S.V. and T.F.O. are supported by Fundación La Marato de TV3 (Ref. 20144330). T.F.O. is supported by the Deutschen Forschungsgemeinschaft Center for Nanoscale Microscopy and Molecular Physiology of the Brain and by SFB1286. S.V. is supported by Ministerio de Economía y Competitividad (MINECO) (BIO2016-78310-R). J.S. is supported by MINECO (BFU2016-78232-P) and Gobierno de Aragón (E45_17R). E.D. is supported by Instituto de Salud Carlos III (PH613883/ERDF/ESF). J.G. and X.S. are supported by MINECO (BIO2015-70092-R) and the European Research Council (Contract 648201).

1. Kalia LV, Lang AE (2015) Parkinson's disease. *Lancet* 386:896–912.
2. Fanciulli A, Wenning GK (2015) Multiple-system atrophy. *N Engl J Med* 372: 1375–1376.
3. Spillantini MG, Crowther RA, Jakes R, Hasegawa M, Goedert M (1998) Alpha-synuclein in filamentous inclusions of Lewy bodies from Parkinson's disease and dementia with Lewy bodies. *Proc Natl Acad Sci USA* 95:6469–6473.
4. Luk KC, et al. (2012) Pathological α-synuclein transmission initiates Parkinson-like neurodegeneration in nontransgenic mice. *Science* 338:949–953.
5. Winner B, et al. (2011) In vivo demonstration that alpha-synuclein oligomers are toxic. *Proc Natl Acad Sci USA* 108:4194–4199.
6. Fellner L, Jellinger KA, Wenning GK, Stefanova N (2011) Glial dysfunction in the pathogenesis of α-synucleinopathies: Emerging concepts. *Acta Neuropathol* 121: 675–693.
7. Bendor JT, Logan TP, Edwards RH (2013) The function of α-synuclein. *Neuron* 79: 1044–1066.
8. Spillantini MG, et al. (1997) Alpha-synuclein in Lewy bodies. *Nature* 388:839–840.
9. Lázaro DF, et al. (2014) Systematic comparison of the effects of alpha-synuclein mutations on its oligomerization and aggregation. *PLoS Genet* 10:e1004741.
10. Silva BE, Einarsdóttir O, Fink AL, Uversky VN (2011) Modulating α-synuclein misfolding and fibrillation in vitro by agrochemicals. *Res Rep Biol* 2:43–56.
11. Pujols J, et al. (2017) High-throughput screening methodology to identify alpha-synuclein aggregation inhibitors. *Int J Mol Sci* 18:E478.
12. Ahsan N, Mishra S, Jain MK, Surolia A, Gupta S (2015) Curcumin pyrazole and its derivative (N-(3-nitrophenylpyrazole) purcumin inhibit aggregation, disrupt fibrils and modulate toxicity of wild type and mutant α-synuclein. *Sci Rep* 5:9862.
13. Barria MA, Gonzalez-Romero D, Soto C (2012) Cyclic amplification of prion protein misfolding. *Methods Mol Biol* 849:199–212.
14. Jung BC, et al. (2017) Amplification of distinct α-synuclein fibril conformers through protein misfolding cyclic amplification. *Exp Mol Med* 49:e314.
15. Herva ME, et al. (2014) Anti-amyloid compounds inhibit α-synuclein aggregation induced by protein misfolding cyclic amplification (PMCA). *J Biol Chem* 289:11897–11905.
16. Tuttle MD, et al. (2016) Solid-state NMR structure of a pathogenic fibril of full-length human α-synuclein. *Nat Struct Mol Biol* 23:409–415.
17. Madadkar-Sobhani A, Guallar V (2013) PELE web server: Atomistic study of biomolecular systems at your fingertips. *Nucleic Acids Res* 41:W322–W328.
18. Salomon-Ferrer R, Case DA, Walker RC (2013) An overview of the Amber biomolecular simulation package. *Wiley Interdiscip Rev Comput Mol Sci* 3:198–210.
19. Genheden S, Ryde U (2015) The MM/PBSA and MM/GBSA methods to estimate ligand-binding affinities. *Expert Opin Drug Discov* 10:449–461.
20. Johnson ER, et al. (2010) Revealing noncovalent interactions. *J Am Chem Soc* 132: 6498–6506.
21. van Ham TJ, et al. (2008) *C. elegans* model identifies genetic modifiers of alpha-synuclein inclusion formation during aging. *PLoS Genet* 4:e1000027.
22. Hamamichi S, et al. (2008) Hypothesis-based RNAi screening identifies neuroprotective genes in a Parkinson's disease model. *Proc Natl Acad Sci USA* 105:728–733.
23. Brenner S (1974) The genetics of *Caenorhabditis elegans*. *Genetics* 77:71–94.
24. Kim H, et al. (2018) The small GTPase RAC1/CED-10 is essential in maintaining dopaminergic neuron function and survival against alpha-synuclein-induced toxicity. *Mol Neurobiol* 55:7533–7552, and erratum (2018) 55:7553–7554.
25. Perni M, et al. (2017) A natural product inhibits the initiation of α-synuclein aggregation and suppresses its toxicity. *Proc Natl Acad Sci USA* 114:E1009–E1017, and erratum (2017) 114:E2543.
26. Ehrnhoefer DE, et al. (2008) EGCG redirects amyloidogenic polypeptides into unstructured, off-pathway oligomers. *Nat Struct Mol Biol* 15:558–566.
27. Bieschke J, et al. (2010) EGCG remodels mature alpha-synuclein and amyloid-beta fibrils and reduces cellular toxicity. *Proc Natl Acad Sci USA* 107:7710–7715.
28. Abbas S, Wink M (2010) Epigallocatechin gallate inhibits beta amyloid oligomerization in *Caenorhabditis elegans* and affects the daf-2/insulin-like signaling pathway. *Phytomedicine* 17:902–909.
29. Gidalevitz T, Krupinski T, Garcia S, Morimoto RI (2009) Destabilizing protein polymorphisms in the genetic background direct phenotypic expression of mutant SOD1 toxicity. *PLoS Genet* 5:e1000399.
30. Sulston J, Dew M, Brenner S (1975) Dopaminergic neurons in the nematode *Caenorhabditis elegans*. *J Comp Neurol* 163:215–226.
31. Harrington AJ, Yacoubian TA, Slone SR, Caldwell KA, Caldwell GA (2012) Functional analysis of VPS41-mediated neuroprotection in *Caenorhabditis elegans* and mammalian models of Parkinson's disease. *J Neurosci* 32:2142–2153.
32. Cao S, Gelwix CC, Caldwell KA, Caldwell GA (2005) Torsin-mediated protection from cellular stress in the dopaminergic neurons of *Caenorhabditis elegans*. *J Neurosci* 25: 3801–3812.
33. Tatenhorst L, et al. (2016) Fasudil attenuates aggregation of α-synuclein in models of Parkinson's disease. *Acta Neuropathol Commun* 4:39.
34. Moree B, et al. (2015) Small molecules detected by second-harmonic generation modulate the conformation of monomeric α-synuclein and reduce its aggregation in cells. *J Biol Chem* 290:27582–27593.
35. Wagner J, et al. (2013) Anle138b: A novel oligomer modulator for disease-modifying therapy of neurodegenerative diseases such as prion and Parkinson's disease. *Acta Neuropathol* 125:795–813.
36. Iljina M, et al. (2016) Kinetic model of the aggregation of alpha-synuclein provides insights into prion-like spreading. *Proc Natl Acad Sci USA* 113:E1206–E1215.